



HAL
open science

Optical and structural performance of the Al/Zr reflection multilayers in the 17-19nm region

Qi Zhong, Wenbin Li, Zhong Zhang, Jingtao Zhu, Qiushi Huang, Haochuan Li, Zhanshan Wang, Philippe Jonnard, Karine Le Guen, Jean-Michel André, et al.

► **To cite this version:**

Qi Zhong, Wenbin Li, Zhong Zhang, Jingtao Zhu, Qiushi Huang, et al.. Optical and structural performance of the Al/Zr reflection multilayers in the 17-19nm region. 2012. hal-00685910

HAL Id: hal-00685910

<https://hal.science/hal-00685910>

Preprint submitted on 6 Apr 2012

HAL is a multi-disciplinary open access archive for the deposit and dissemination of scientific research documents, whether they are published or not. The documents may come from teaching and research institutions in France or abroad, or from public or private research centers.

L'archive ouverte pluridisciplinaire **HAL**, est destinée au dépôt et à la diffusion de documents scientifiques de niveau recherche, publiés ou non, émanant des établissements d'enseignement et de recherche français ou étrangers, des laboratoires publics ou privés.

Optical and structural performance of the Al/Zr reflection multilayers in the 17–19nm region

Qi Zhong¹, Wenbin Li,¹ Zhong Zhang,¹ Jingtao Zhu,¹ Qiushi Huang,¹ Haochuan Li,¹ Zhanshan Wang^{1,*}, Philippe Jonnard,² Karine Le Guen,² Jean-Michel Andr e² Hongjun Zhou³ and Tonglin Huo³

¹Department Institute of Precision Optical Engineering, Department of Physics, Tongji University Shanghai 200092, China

²Laboratoire de Chimie Physique – Matière Rayonnement, UPMC Univ Paris 06, CNRS UMR 7614, 11 rue Pierre et Marie Curie, F-75231 Paris cedex 05, France

³National Synchrotron Radiation Laboratory, University of Science and Technology of China, Hefei 230029, China
[*wangzs@tongji.edu.cn](mailto:wangzs@tongji.edu.cn)

Abstract: Two kinds of Al/Zr (Al(1%wtSi)/Zr and Al(Pure)/Zr) multilayers for extreme ultraviolet (EUV) optics were deposited on fluorine doped tin oxide coated glass by using direct-current magnetron sputtering technology. The comparison of the two systems shows that the Al(1%wtSi)/Zr multilayers have the lowest interfacial roughness and highest reflectivity. Based on the X-ray diffraction, the performance of the two systems is determined by the crystallization of Al layer. To fully understand the Al(1%wtSi)/Zr multilayer, we built up a two-layer model to fit situation of the AFM images, and simulate the grazing incident x-ray reflection measurements of multilayers with various periods (N=10, 40, 60, 80). Below 40 periods, the roughness components are lowered. After 40 periods, both surface and interfacial roughness increase with the period number. According to transmission electron microscope images, the model can represent the variable structure of the system.

References and links

1. A. J. Corso, P. Zuppella, P. Nicolosi, D. L. Windt, E. Gullikson and M. G. Pelizzo, "Capped Mo/Si multilayers with improved performance at 30.4 nm for future solar missions," *Opt. Express*, **19**(15), 13963–13973 (2011).
2. S. Bajt, J. B. Alameda, T. W. Barbee Jr., W. M. Clift, J. A. Folta, B. Kaufmann, E. A. Spiller, "Improved reflectance and stability of Mo-Si multilayers," *Opt. Eng.*, **41**(8), 1797–1804 (2002).
3. D. L. Windt, J. A. Bellotti, "Performance, structure, and stability of SiC/Al multilayer films for extreme ultraviolet applications," *Appl. Opt.*, **48**(26), 4932–4941 (2009).
4. P. Jonnard, K. L. Guen, M.-H. Hu, J.-M. Andr e E. Meltchakov, C. Hecquet, F. Delmotte, A. Galtayries, "Optical, chemical and depth characterization of Al/SiC periodic multilayers," *Proc. of SPIE*, **7360**, 73600O 1-9 (1997).
5. E. Meltchakov, C. Hecquet, M. Roulliay, S. D. Rossi, Y. Menesguen, A. J rome, F. Bridou, F. Varniere, M.-F. Ravet-Krill, F. Delmottel, "Development of Al-based multilayer optics for EUV," *Appl. Phys. A*, **98**, 111–117 (2010).
6. M.-H. Hu, K. L. Guen, J.-M. Andr e P. Jonnard, E. Meltchakov, F. Delmotte, A. Galtayries, "Structural properties of Al/Mo/SiC multilayers with high reflectivity for extreme ultraviolet light", *Opt. Express*, **18**(19), 20019–20028 (2010).
7. J. T. Zhu, S. K. Zhou, H. C. Li, Q. S. Huang, Z. S. Wang, K. Le. Guen, M.-H. Hu, J.-M. Andr e P. Jonnard, "Comparison of Mg-based multilayers for solar He II radiation at 30.4 nm wavelength," *Appl. Opt.*, **49**(20), 3922–3925 (2010).
8. K. Le Guen, M.-H. Hu, J.-M. Andr e S. K. Zhou, H. Ch. Li, J. T. Zhu, Z. S. Wang, C. Meny, A. Galtayries, P. Jonnard, "Observation of asymmetry when introducing Zr in Mg/Co multilayers," *Appl. Phys. Lett.* **98**, 251909 (2011)
9. K. Le Guen, M.-H. Hu, J.-M. Andr e P. Jonnard, S. K. Zhou, H. Ch. Li, J. T. Zhu, Z. S. Wang, "Development and interfacial characterization of Co/Mg periodic multilayers for the EUV range," *J. Phys. Chem. C*. **114**(14), 6484–6490(2010).

10. D.L. Voronov, E.H. Anderson, R. Cambie, S. Cabrini, S.D. Dhuey, L.I. Goray, E.M. Gullikson, F. Salmassi, T. Warwick, V.V. Yashchuk, and H.A. Padmore, "A 10,000 groove/mm multilayer coated grating for EUV spectroscopy," *Opt. Express*, **19**(7), 6320–6325 (2011).
 11. S. B. Qadri, C. Kim, M. Twigg, D. Moon, "Ion-beam deposition of Zr-Al multilayers and their structural properties," *Surf. Coat. Technol.*, **54**(55), 335–337 (1992).
 12. J-K. Ho, K-L. Lin, "The Structure of Compositionally Modulated Al-Zr Multilayer films," *Scripta Metallurgica et Materialia*, **33**(12), 1895–1990 (1995).
 13. J-K. Ho, K-L. Lin, "The metastable Al/Zr alloy thin films prepared by alternate sputtering Deposition," *J. Appl. Phys.*, **75**(5), 2434–2440 (1994).
 14. K.J. Blobaum, T.P. Weihs, T.W. Barbee, Jr., M.A. Wall, "Solid state reaction of Al and Zr in Al/Zr multilayers: a calorimetry study," UCRL, J C–118965 (1995).
 15. H. Nii, M. Niibe, H. Kinoshita, Y. Sugie, "Fabrication of Mo/Al multilayer films for a wavelength of 18.5nm," *J. Synchrotron Rad.*, **5**, 702–704 (1998).
 16. H.Nii, M.Miyagawa, Y. Matsuo, Y. Sugie, M. Niibem, H. Kinoshita, "Control of Roughness in Mo/Al Multilayer Film Fabricated by DC Magnetron Sputtering," *Jpn. J. Appl. Phys.*, **41**, 5338–5341 (2002).
 17. D. G. Stearns D. P. Gaines, D. W. Sweeney, E. M. Gullikson "Nonspecular x-ray scattering in a multilayer-coated imaging system," *J. Appl. Phys.*, **84**(2), 1003–1028 (1998).
 18. M. Trost, S. Schröder, T. Feigl, A. Duparré A. Tünnemann, "Influence of the substrate finish and thin film roughness on the optical performance of Mo/Si multilayers," *Appl. Opt.*, **50**(9), C148–153 (2011).
 19. D. L. Windt, "IMD–Software for modeling the optical properties of multilayer films," *Comput. Phys.* **12**(4), 360–370 (1998).
 20. Q. Yang, L.R. Zhao, "Characterization of nano-layered multilayer coatings using modified Bragg law," *Materials Characterization*, **59**, 1285–1291 (2008).
-

1. Introduction

With the research of reflecting multilayer coatings in the extreme ultraviolet (EUV) spectral region, preference is often given to the Mo/Si multilayers as the most advanced technological levels. However, with the increasing absorption of Si at longer wavelength region below Si L–edge, the reflectivity of Mo/Si multilayers falls gradually and the spectral bandwidth also becomes relatively wide [1–2]. In principle, other material combinations can provide higher reflectivity and narrower bandwidth than Mo/Si multilayers at the long wavelength region. Therefore, some researchers have investigated Al–based [3–6] and Mg–based [7–9] systems, for which absorption edges are located at 17.1 nm and 25 nm, respectively.

For the Al–based system, there are many promising material combinations, such as Al/Mo, Al/Y, Al/Zr, Al/SiC, etc. However, the inhomogeneous crystallization of aluminum and the interdiffusion in the multilayers influence the performance of the Al–based system. As compared with the Si–based, Al–based and Mg–based multilayers [3–9], the Al/Zr system is another candidate Al–based multilayer that shows good theoretical performance in the EUV region. The highest reflectivity in the Al–based multilayer makes it especially attractive for the EUV applications, such as high reflectivity coatings [3] and blazed multilayer grating structure [10]. Therefore, scientists have focused on the Al/Zr multilayer since the end of the last decade. Because the intermediate compounds are formed by Al and Zr materials, the structure and composition of thick Al/Zr multilayer (i.e., the thickness of one layer is over 100nm) have been investigated [11–14]. It was shown that the structure of thick Al/Zr multilayer was influenced by the coating process and the crystalline states of Al and Zr layers. Additionally, the interfacial structure was also affected by the temperature and time factors. While a relatively good reflectivity was shown for Al/Zr multilayer coated on the grating in the EUV region [3, 10], no data is found on the optical and structural performance of the Al/Zr system in the wavelength region of 17–19nm.

In this paper, we report on the performance of periodic Al/Zr multilayer designed for use as EUV high reflectivity mirrors in the range of $\lambda \sim 17\text{--}19\text{nm}$. The deposition processes of multilayer are outlined in Sec.2. In Sec.3–1, we compare two different multilayer types (Al(1%wtSi)/Zr and Al(Pure)/Zr) with different periods. The structural properties were studied by using grazing incident X–ray reflection (GIXR), X–ray diffraction (XRD) and

near-normal incident EUV reflectance. We find that the doping in Al layer influence the performance of the Al/Zr system. To fully estimate the Al(1%wtSi)/Zr periodic multilayer, we built up a two-layer model to explain the AFM images, and simulate the GIXR measurements. The effect of the period number is discussed in the Sec.3-2. The model seems relatively suitable to characterize the structure of multilayer and is confirmed by the cross-section TEM. We conclude in Sec.4 with comments regarding the performance for the Al/Zr system.

2. Experimental

All samples were fabricated by direct-current magnetron sputtering technology [7], under the base pressure 8.0×10^{-5} Pa. The sputter gas was Ar with purity of 99.999%, and the gas pressure was held constantly at 1.35 ± 0.02 mTorr (0.180Pa). The substrate was fluorine doped tin oxide coated glass (FTO). The targets of zirconium (99.5%) and silicon doped aluminum (Al(1%wtSi)) or aluminum (99.999%, Al(Pure)) with diameter of 100 mm were used. By magnetron sputter deposition, a series of multilayers were fabricated in which the period numbers of Al(1%wtSi)/Zr were varied from 10 to 80 and the period numbers of Al(Pure)/Zr were held at 40 and 60. In order to observe the cross section of the multilayers, Al(1%wtSi)/Zr (N=120) was prepared on Si(100) substrate.

For characterizing the structure of the samples, the GIXR was performed by using a Cu K α source ($\lambda=0.154$ nm). The modified Bragg law was used to calculate the multilayer period thickness for all the samples. The measurements provided identification of crystalline phases present in the modified layer along with structural changes during the different period numbers on the FTO substrates. The surface roughness and micrographs were also measured with a Veeco, DI 3100 scanning probe microscope, operated in AFM mode. For estimating the interfacial microstructure and periodic structure of Al(1%wtSi)/Zr system, the scanning transmission electron microscope (TEM, FEI Tecnai G² F20) was used on the specimen prepared by focused ion beam (FIB) etching using in the Materials Analysis Technology Ltd.

The near-normal incident EUV reflectance was made at a 5° incident angle, using the reflectometer on the Spectral Radiation Standard and Metrology Beamline and Station (beamline U26) at the National Synchrotron Radiation Laboratory in Hefei, China. An aluminum filter was inserted into the incident light beam to remove the high order radiation.

3. Results and discussion

3.1 Al (1%wtSi)/Zr and Al (Pure)/Zr multilayers

In order to estimate the influence of Si doping in the Al layers [4-6], we firstly compare two systems of Al (1%wtSi)/Zr and Al (Pure)/Zr with the same period numbers (40 and 60). The interface quality of the multilayers are characterized by GIXR and shown in Fig. 1. The period thicknesses are 8.96, 9.15, 8.96 and 9.03nm for Al(1%wtSi)/Zr-N40, Al(1%wtSi)/Zr-N60, Al(Pure)/Zr-N40 and Al(Pure)/Zr-N60, respectively. For both Al(1%wtSi)/Zr systems, the curves show sharp Bragg peaks which indicate smooth interfaces. However, Al(Pure)/Zr multilayers have lower reflectivity with the increasing incident angle compared to Al(1%wtSi)/Zr, especially for period number of 60 in the Fig. 1(b). The phenomenon shows that the roughness of Al(Pure)/Zr might be larger than that of Al(1%wtSi)/Zr. Therefore, the EUV reflectance measurements are required to further characterize the two systems. While similar theoretical reflectance is obtained for the two systems in the Fig. 2(a), the real performance of Al(Pure)/Zr multilayers turns out to be worse. The measured peak reflectance of periods 40 and 60 are only 37.9% and 33.2%, while the values in Al(1%wtSi)/Zr system are 41.2% and 37.8%, respectively. The lower reflectance of Al(Pure)/Zr multilayers indicate the poor interface structure in this multilayer system, which is consistent with the conclusion of GIXR results.

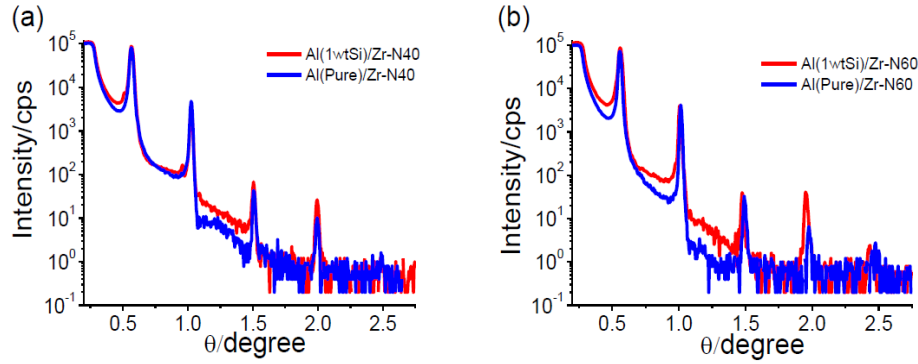


Fig.1 Grazing incidence x-ray reflectivity curves of two multilayer types. a: Al(1%wtSi)/Zr (40 periods, red line) and Al(Pure)/Zr (40 periods, blue line); b: Al(1%wtSi)/Zr (60 periods, red line) and Al(Pure)/Zr (60 periods, blue line).

To identify the reason of different interfacial structure, we did the XRD measurements on different systems with the same acquisition time and the incident beam flux, which are shown in Fig. 2(b). For all samples, three peaks (fcc Al $\langle 111 \rangle$, hcp Zr $\langle 002 \rangle$ and $\langle 101 \rangle$) are present. In both 40 and 60 periods, the peak heights of Al $\langle 111 \rangle$ in the Al(Pure)/Zr system are higher than those of the Al(1%wtSi)/Zr system. The Al(Pure) layer has an intact crystallization, but the crystallization of Al(1%wtSi) layer could be worse due to Si. Taking the other similar conditions of two systems into account, the crystallization of Al layers could contribute to the interfacial roughness. Therefore, the presence of Si, even in a small proportion, would disfavor the crystallization of Al layer and smooth the interface, which is consistent with some researches [4–6]. Contrary to the situation of Al $\langle 111 \rangle$, the Zr $\langle 002 \rangle$ and $\langle 101 \rangle$ peaks have higher peak heights in the Al(1%wtSi)/Zr system with period number of 60. The crystallization of Zr layer could also be influenced by the material Si in Al (1%wtSi)/Zr samples. So the material Si might enhance the crystallization of Zr layer and decrease the interfacial roughness. Because the Al and Zr formed immediate compounds [10], the peak curves of Al and Zr phases are not similar, which might due to the large interface thickness in the interlayer. From the above results, it can be seen that a small proportion of silicon in Al layer has a strong effect on the interfacial roughness of the two systems, where Al(1%wtSi)/Zr multilayers have smoother interfacial roughness than that of Al(Pure)/Zr. Therefore, we decide to focus on Al(1%wtSi)/Zr system to characterize its performance.

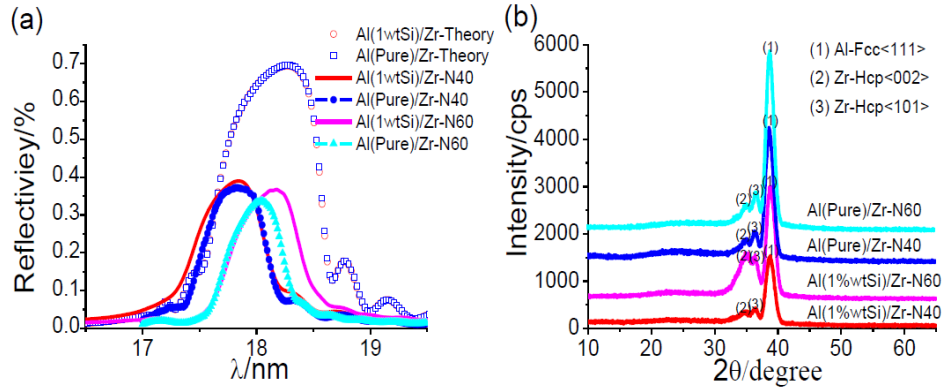


Fig.2 (a) Calculated reflectivity around 18 nm for two systems at normal incidence (points), the curves of experiment for Al (1%wtSi)/Zr (red solid line) and Al (Pure)/Zr (blue line and symbol) are also present; (b) diffraction curves of the samples of Al(1%wtSi)/Zr (red line) and Al(Pure)/Zr (blue line) with different period numbers (40, 60).

3.2 The performance of Al (1%wtSi)/Zr multilayer

In the previous section, we find that the crystallization of Al and Zr layer leads to different diffraction peaks in curves of Al(1%wtSi)/Zr multilayer with 40 and 60 periods (as shown in Fig. 2(b)). In the Al-based system, the surface roughness is influenced by the crystallization of Al layer and period numbers [15, 16]. Therefore, to estimate the Al(1%wtSi)/Zr multilayer, four samples of various period numbers (N=10, 40, 60, 80) were prepared and characterized by AFM, which are measured in the $10\mu\text{m}\times 10\mu\text{m}$ area as shown in Fig. 3. Before coating, the FTO substrate roughness is 0.71nm. After coating various period numbers (N=10, 40, 60, 80), the values are 0.40nm, 0.40nm, 0.54nm and 0.82nm, respectively. The surface of the 10 and 40 periods' samples consist of sparsely packed small particles and smooth the surface. However, over 40 periods, the surface become much rougher, and has densely packed particles. Considering the roughness evolution in the Mo/Si multilayers [17, 18] and Al-based systems [15, 16], the crystal size of the metal layer is smaller than the roughness of substrate. The roughness component is smoothed through the multilayers before the saturation value of the number of periods. On the contrary, the crystal size is larger than the roughness of substrate, and the roughness increases with the period number. From the AFM images, we can see that the substrate roughness decreases and smoothens through the multilayer below saturation period N=40 of Al (1% wtSi)/Zr multilayers (i.e., calculated by the IMD [19]). After 40 periods, the roughness is larger than 0.40nm, and increases with the period number.

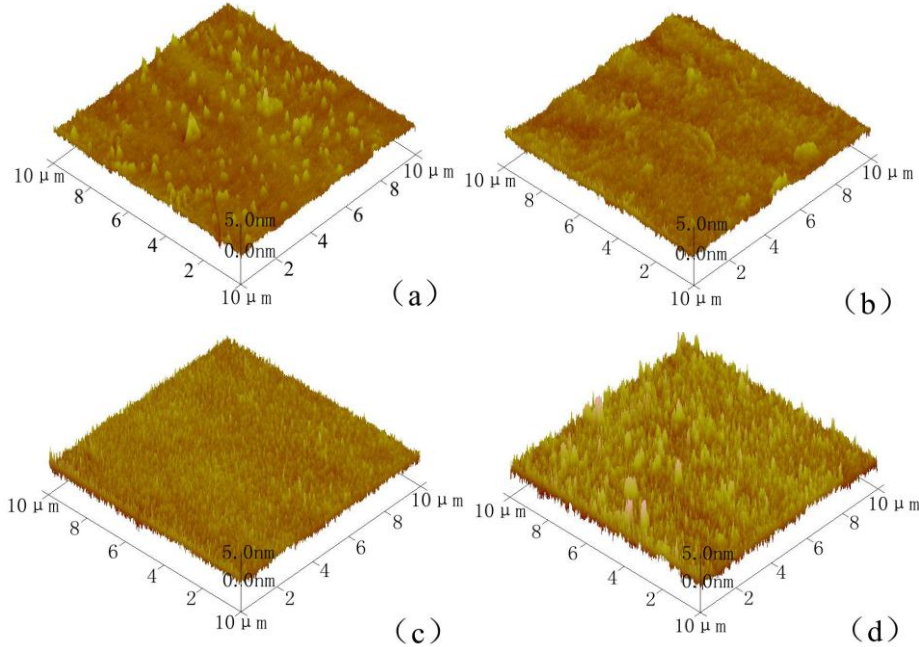


Fig.3 AFM images of Al (1%wtSi)/Zr multilayer films with various layers, N10(a), N40(b), N60(c), N80(d).

To identify the different interfacial roughness evolution as a function of the number of periods, the GIXR is used. The simulation of the curves is based on the program, which adopts the two-layer model that is to say the multilayer is considered as the alternation of only Al and Zr layers. In addition a ZrO_2 capping layer is added at the top of the stack. Calculation is made by a differential evolution algorithm [20]. In the system, the interfacial roughness has different trends before and after 40 periods, which is consistent with the results of AFM images. Thus, the roughness is estimated before and after 40 periods by using the following equations:

$$\sigma = \begin{cases} B_1 + A_1 \exp(-N/C_1) & 0 < N \leq 40 \\ B_2 + A_2 \exp(N/C_2) & N > 40 \end{cases}$$

where σ is the root-mean square (rms) value of the interfacial roughness, and B_1 , A_1 , C_1 and B_2 , A_2 , C_2 are the parameters correlated with the interfacial roughness. The parameter N is number of periods. For simulating GIXR in the Fig. 4(a), parameters A_1 , A_2 represent the slope of the changing trend, and the B_1 , B_2 can be influenced by the substrate roughness and the surface roughness of 40 periods. For samples with 10 and 40 periods, the parameters B_1 are 0.13 and 0.39; A_1 are 0.57 and 0.31; C_1 are 13.24 and 8.29, respectively. Thus, the substrate roughness is lowered by the multilayers and the capability of smoothing increases with period number. However, over 40 periods, the roughness increases with the period number. For example, the roughness parameters in the 80 periods sample are 0.31, 0.39, 13.24, 0.27 and -0.10, 65.33 for A_1 , B_1 , C_1 , A_2 , B_2 and C_2 respectively. From the Fig. 4(a), the simulation data can be best fitted the GIXR measurements. From the data, we can assume that the multilayer might have a smooth interface with a lower roughness below 40 periods. But after 40 periods, the roughness is accumulated with the period numbers, which might have the rough interface in the multilayer.

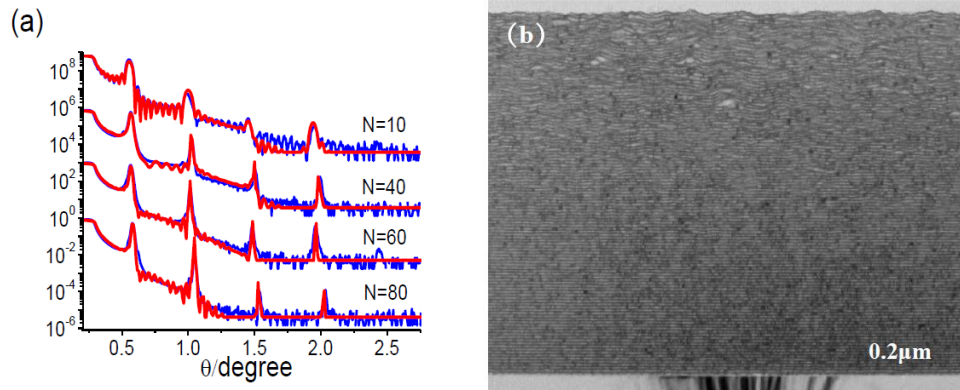


Fig.4 (a) X-ray reflectivity measurements color curve (blue line) of the different period number and curves obtained by a fitting calculation (red line); (b) Transmission electron micrograph of the Al (1%wtSi)/Zr multilayer (N120) obtained with low magnification.

To confirm the microstructural changes, which might be connected with the changes in GIXR and AFM in the different samples, TEM measurements have been performed on different scales in Fig. 4(b) and Fig. 5. Shown in Fig. 4(b) is the low magnification transmission electron micrograph of a cross-section, where the alternately stacked layers of Zr and Al(1%wtSi) are represented as black and white area, respectively. Because Al and Zr materials can formed many intermediate compounds, the interlayers could be consisted of an amorphous Al-Zr alloy, which would contribute along with interfacial roughness to the interfacial total width [10, 14]. In Fig. 4(b), the multilayer shows a variable film structure with the increasing period numbers. From bottom layer to the 90th period, the multilayer has a good alternating thin film structure. After 90th period, the structure becomes obviously rougher. To investigate the microstructural changes at the different periods of layers, the high magnification transmission electron micrographs (TEM) and selected area electron diffraction (SAED) pattern are performed and shown in Fig. 5. Three areas with 40th, 60th and 80th period are characterized in the specimen. From the Fig. 5(a, c), the lower layers (40th period) have smooth interfaces and good multilayer qualities, while the situations of upper layers (80th period) are worse. In Fig. 5(f), the Al<111> peak can be observed clearly, which is represented as the out-of-plane (i.e., along the growth direction) [3]. But at 80th period in Fig. 5(d), it could not growth along the same direction. We could see that the interface quality and

interfacial structure become much worse in the large periods. In the SAED (Fig. 5(g-i)) pattern, as the obviously changes in the Al<111> peak, the Nano beam diffraction (NBD) of the lower layers (40th period) shows crystals of the region ($\sim 0.1\mu\text{m}$) highly oriented. For the areas 60th and 80th period, the NBD indicates that crystals deviate about 10.42° , and 28.06° , respectively. The reason is that every diffraction point in the SAED image represents a series of lattice planes in the film. For small period, the film can decrease the substrate roughness, and the lattice planes are parallel to the substrate plane. So the diffraction points are concentrated. However in the large periods, the roughness of the metal layer increases with the period numbers. The layers become much bent from the substrate, which are represented as a number of different angles (such as 10.42° , and 28.06°) of the lattice planes in the film. So the diffraction points follow by divergence. From the reason, the film has a smooth interface and highly oriented crystals below 40th period, showing very promising optical and structural performance. But after 40th period, the interface quality becomes worse. The interfacial roughness is accumulated with increasing the period number and leads to an increase of surface roughness. We can conclude that the simulation model mentioned above could represent the variable structure of the Al (1% wtSi)/Zr system.

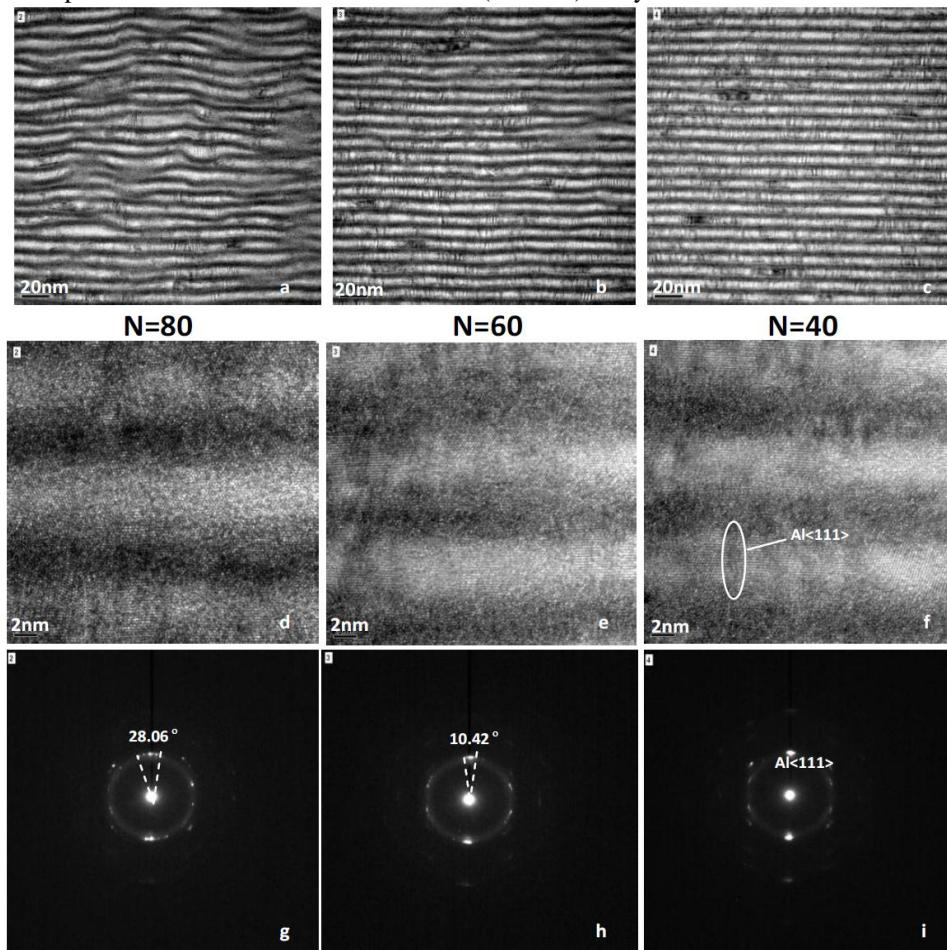


Fig.5 High magnification transmission electron micrographs and selected area electron diffraction pattern used to observed the cross-section of Al(1%wtSi)/Zr multilayer (N120). The micrographs and SAED patterns of the periods N=80 (a, d, g), N=60 (b, e, h) and N=40 (c, f, i) are shown in the figure.

4. Conclusion

We report on the two systems, Al(1%wtSi)/Zr and Al(Pure)/Zr multilayers, designed for the EUV region. It is found that the Al(1%wtSi)/Zr multilayers have lower interfacial roughness and smoother interface because of the doping in Al layer. The EUV reflectivity has revealed significantly improved performance of the Al(1%wtSi)/Zr multilayer compared to Al (Pure)/Zr. The peaks of Al(1%wtSi)/Zr multilayers are 41.2% and 37.8% for multilayers with 40 and 60 periods, respectively, which are higher than the values of Al(Pure)/Zr multilayers. From the analysis of XRD, it has been demonstrated that the presence of Si could influence the crystallization of both Al and Zr layers and smooth the interface, which contributes to the small interfacial roughness and high performance of Al(1%wtSi)/Zr multilayers.

In order to characterize roughness evolution of the Al(1%wtSi)/Zr system, four periodic multilayers were deposited on the FTO and measured by AFM. We built up a two-layer model to simulate the GIXR measurements, which would represent the variable structure of the multilayers. From the AFM images and GIXR fitting data, the interfacial roughness reveals different trends in the periodic multilayers. With less than 40 periods, the roughness components are smoothed by the multilayers, while surface roughness was 0.40nm at 40 periods. However, for more than 40 periods, the surface and interfacial roughness were accumulated with the increasing period number. Because the crystals in different periods have the different growth directions from analysis of the TEM and SAED, the layers show the different interface quality in the multilayer, which can verify the assumption of the simulation model in GIXR. Therefore, the performance of the Al(1%wtSi)/Zr multilayer below 40 periods should be optimized in further application. Considering the reason of interfacial roughness in the Al(1%wtSi)/Zr system, the phase and chemical composition of the interlayer will be the crucial problem to the system.

Acknowledgments

This work is supported by National Basic Research Program of China (No. 2011CB922203), National Natural Science Foundation of China (No.10825521, 11061130549).